

Notes by Les Fishbone for Summarizing the Zel'dovich and Novikov Textbook, *The Structure and Evolution of the Universe*

Les Fishbone

(Transcribed by T. G. Throwe)

(Dated: June - October 2022)

INTRODUCTION

A. Well-Established

- Observed isotropy of Universe to $\lesssim 0.1 - 1.0\%$ via relic radiation
- Homogeneity deviations $\lesssim 0.1 - 1.0\%$ on a scale of 10^{10} ly
- GTR with cosmo constant is the best basis
- Steady state and changing G are not valid
- Hubble parameter is 50 km/sec/Mpc to within 50%
- Uniform density and pressure
- With $\Lambda \sim 0$, critical density is $0.510^{-29} g/cm^3$
- If density \downarrow critical, Universe will expand unbounded and is infinite
- Density is important to know
- The use of celestial objects of a given type to determine the structure of the Universe is complicated by their intrinsic evolution and the evolution of their number as a function of time
- “But the distances over which galaxies can be observed are small compared to cosmological scales. To this day, therefore, the structure of the Universe has not been established through observations of ordinary galaxies either.”
- Important to know average density and particle types
- Luminous matter has an average density of $\sim 10^{-31} g/cm^3$, suggesting average number density of baryons $\sim 6 \times 10^{-8} /cm^3$
- Galaxy motions suggest dark matter
- Antimatter absence suggests charge asymmetry

- RR photons now have an average number density of $\sim 400/cm^3$, $10^8 - 10^{10}$ more than the number density of baryons. Their T of 2.7 K corresponds to an energy of 0.0007eV, yielding an overall photon mass-energy density now of $5 \times 10^{-34} g/cm^3$, much lower than that of baryons now.
- Density of neutrinos and gravitational waves is difficult to determine.
- Thus there is as yet no answer to whether total density now is greater or less than critical density, and consequently whether Universe is finite or infinite.
- Going back in time, T increases and radiation and matter are in thermo equilibrium because matter density $\sim V^{-1}$, while radiation density $\sim V^{-4/3}$
- At $t \sim 1\text{sec}$ in Friedmann solution, $T \sim 10^{10}$ or 10^6eV and matter density $\sim 10^6 g/cm^3$. There would have been photons plus electrons and positrons and protons and neutrons.
- Expansion leads to disappearance of positrons, while neutrons decay or combine with protons, forming 70% hydrogen and 30% helium by mass, but almost no heavier elements. Also remaining were neutrinos and antineutrinos.
- Further expansion means matter mass density exceeds photon mass-energy density of photons.
- All RR now seen is from $z \sim 1000$, the time of last scattering. The corresponding distance is about 97% of the distance to the singularity, the horizon distance. The observable volume is then about 90% of the maximum possible volume.
- Existing structure indicates early deviations from homogeneity and isotropy.

B. Not Well-Established

- Use perturbation theory by modes on simple time-dependent solution rather than exact solutions of four dimensional spacetime, especially since initial conditions are unknown.

- But how large were density perturbations?
- Present average density of galaxy clusters is roughly characteristic of the average overall density at their formation time; this leads to an estimation of the formation time. For the plasma state in the RD era, this leads to fractional density oscillations of 10^{-3} for $\delta\rho/\rho$
- With theory, observations of RR fluctuations then permit estimation perturbation magnitude was functions of the scale or mass, i.e., the perturbation spectrum.
- Summary of Important Recent Result: Universe picture represents a weakly perturbed (almost homogeneous) expanding Universe with a definite initial (and large) entropy. Measurements of the spectrum and spatial distribution of the RR support this picture.
- But can this picture explain galaxy rotation, magnetic fields and the origin of quasars?
- Primordial magnetic fields are not necessary; plasma motions can generate observed fields.
- But galaxy rotation given vortex-free initial perturbations? Possible given galaxy interactions.
- Another theory is that galaxies formed from explosions of hyper dense bodies, but this violates known physics.

C. Beginning of Expansion

- Anisotropic expansion before $t \sim 1\text{sec}$?
- Is there infinite density at the beginning or is that a characteristic of the isotropic homogeneous model?
- There is proof a singularity even if expansion was not homogeneous and isotropic?
- Details later, but here consider here aforementioned models plus perturbations. With these bases, do present observations and the laws of physics permit the establishment of the history of the Universe, including after and before (if meaningful) the singularity and the nature of the singularity itself?
- Approach this via thermodynamics: many initial states can lead to a the same final state, which can serve as the new initial state for further evolution; the actual initial state is forgotten.
- Thus find that cosmo model which arises from a wide class of initial early states.

- Many anisotropic lead to isotropic expansion. But are such statistical arguments applicable?
- Why is the entropy of the Universe large? Why hot at the start of expansion? Why are perturbations leading to observed structure of just the correct magnitude?
- Laws of physics seem sufficient to explain all. Intense particle creation can occur from intense gravitational field close to the time right after the singularity, but only given anisotropic expansion.
- Finally, there can be new phenomena given quantization of the metric.
- Historical remark: Friedmann theory 1922-1924; Einstein mention thereof; Lemaitre 1927. Thus Lemaitre did not “independently” establish the laws of the expanding Universe.
- After Hubble discovery in 1929, math solutions became established theory. Einstein remarked in 1931 that Friedmann was the first to follow this way;

I. THE HOMOGENEOUS, ISOTROPIC UNIVERSE: ITS EXPANSION AND GEOMETRICAL STRUCTURE

1. Local Properties of the Homogeneous, Isotropic Cosmological Model

Standard exposition based on Newtonian theory for Hubble expansion, age of the universe, and matter density and pressure

2. Relativistic Theory of the Homogeneous, Isotropic Universe

GTR needed to analyze large regions

See Vol. 1 for a sufficient exposition of GTR; Theory of Fields by Landau and Lifschitz for a complete GTR \gg Friedmann eqns, with results the same as for the Newtonian description

Various models for open, closed, and flat (critical density) geometry

3. The Propagation Of Photons And Neutrinos; Observational Methods For Testing Cosmological Theories

Significant effects of relativistic matter on early expansion; cosmological neutrinos would not be observable today, though photons are

As density becomes infinite as size and age approach zero, visibility to an earlier stage is not possible because the optical depth, dependent on particle density, diverges.

Whereas the theoretical particle horizon is at $t = 0$, practically it is at a later time when the optical depth is of order unity.

Observational quantities: red shift, angular size and luminosity of distant objects, amount of matter as a function of red shift, apparent magnitude

Deceleration parameter and the first approximation

Impossibility of determining the cosmo model if sources evolve in an unknown way

Distance ladder to far-away objects

Redshift vs. apparent magnitude observations rule out steady-state universe

No Olbers paradox in an expanding universe

Complete EM spectrum in the universe, of which a small section is the RR (Fig. 27, p. 126)

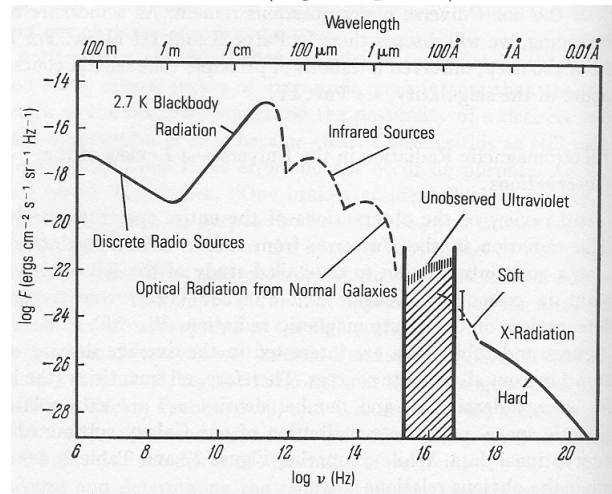


FIG. 27.—The spectrum of electromagnetic radiation in the Universe

4. The Cosmological Constant

Cosmo constant would only be manifest on the scale of the universe

History of cosmo constant starting with opinion that universe is static; Einstein desire for corresponding GTR solution and ideas of Mach

Hubble observation of expansion and Friedmann non-static GTR solutions Realization that cosmo constant is not needed, especially given new Hubble value of 75 and longer age for universe

Various cosmo models with nonzero cosmo constant.

II. PHYSICAL PROCESSES IN THE HOT UNIVERSE

5. Intro to Part II

Relic radiation (RR = CMB) at $T=2.7$ K is the most important observational fact, and this RR (nor the equivalent background neutrinos) could not have been produced by astronomical objects

Also, there are about $10^{9+/-1}$ photons per baryon

These two data allow characterization of the composition of the Universe at earlier time given thermodynamic equilibrium with specific entropy of matter conserved and volume changing smoothly during expansion

In later stages, nuclear reactions cease and nucleosynthesis takes place, with only photons, electrons, nuclei, neutrinos and gravitons surviving, with the last two undetectable

Hot universe proved by observations for the period $10y \leq t \leq 10^{10}y$, and likely only consisting of mattering the large, not antimatter too.

Short historical review of RR prediction and discovery

6. Thermodynamic Equilibrium...

Early radiation-dominated era with matter and antimatter

Ratio of photons to baryons hardly changes during expansion: thermo equilibrium during early stages and conservation of RR photons later

Given $kT > mc^2$, the number of particles and antiparticles of each kind equals the number of photons. Thus $\sim 10^8$ nucleon-antinucleon pairs in the early universe for each nucleon today. This suggests that the present nucleons result from a small excess (10^{-8}) of nucleons over anti nucleons early.

Expansion eras are therefore:

1. Hadron era: with nucleons and antinucleons and ordinary and anti versions of all other particles; $t \lesssim 10^{-6}s$ and $T > 10^{13}K$
2. Lepton era: with only a small remainder of nucleons, electron and positrons annihilate by the end, leaving a small remainder, and neutrinos decouple; $10^{-6}s < t < 10s$ and $10^{13}K > T > 5 \times 10^9K$
3. Photon-Plasma era: plasma and radiation in equilibrium; $10s < t < 10^{12}s$ and $5 \times 10^9K > T > 10^4K$
4. Post-recombination era: $t > 10^{12}s$ and $T < 10^4K$ when the RR becomes transparent

Gravitons, if they exist, would always be present but would not interact with other particles after Planck time $\sim 10^{-43}s$.

MISSING OR TRANSITION TEXT RESULTING FROM IMAC FAILURE TO BE RESOLVED

At a sufficiently high temperature T such that $kT > Mc^2$, where M is the mass of the most massive particle, photons and other relativistic particles dominate

$P = e/3 = \rho \times c^{2/3}$ and $e = \kappa \times \sigma \times T^4$ to take account of all kinds of relativistic particles.

And $n \sim e/(3kT)$ for the particle density

Consider $T \sim 1\text{MeV}$, $t \sim 1\text{sec}$, and $n(\text{electron}) \sim n(\text{positron}) \sim 10^{-31}\text{cm}^{-3}$ and annihilation cross section $\sigma(\text{Annihilation}) \sim 10^{-24}$ and particles move at c , then time to establish equilibrium is

$\tau \sim 10^{-17}$ small compared to 1 sec.

Similarly for higher mass particles at higher temperatures and correspondingly earlier times.

When $kT > m_{\text{nuc}}c^2$, $n_{\text{nuc then}} - n_{\text{antinuc then}} = n_{\text{nuc now}} \sim 10^{-8} \times n_{\text{photons now}}$

$n_{\text{nuc then}} \sim n_{\text{photons then}}$

One could apply the same considerations to quarks and so on and so forth if $kT > m_q c^2$

Hot vs. cold matter as $n \gg \infty$? Different models of Hagedorn and Omnes

Quark theory for nucleons

Conservation of energy and baryon charge and entropy for slow, adiabatic processes \Rightarrow evolution can be described.

Particle-antiparticle annihilation requires binary collisions, increasingly unlikely as the Universe expands.

1. Residual $n(\text{antiparticle})$ in charge symmetric theory is very small at the end of hadron era, $T \sim 1\text{MeV}$ because annihilation σ is large and nucleon excess \Rightarrow exponentially small $n(\text{antiparticle})$ when their creation ceases.
2. Residual $n(q)$ is large. With respect to photons, it is $\sim [Gm^2/hc]^{1/2} \sim 10^{-18}$; with respect to nucleons, it is about 10^{-9} .
3. In spatially homogeneous, charge-sym universe, nucleon problem similar to quarks and leads to 10^{-18} nucleons/photon, disagreeing with observations by 10^{10} . So we should consider charge-asymmetric universe.

This leads to Omnes theory. Charge symmetry of primordial homogeneity is spontaneously broken on the microscopic scale. Strong interaction leads to separation of matter and antimatter drops of size $\sim 10^{-3}\text{cm}$ at 10^{-6}sec

This separation tendency stops as T decreases and annihilation occurs as usual. But spatial separation means annihilation occurs mainly at the boundary of regions.

There exist regions with 10^{-9} nucleons/photon and regions with 10^{-9} antinuc/photon \Rightarrow galaxies and anti-galaxies. Omnes calculations lead to two characteristic quantities: average $n(\text{nuc or antinuc}) / n(\text{photons})$. And characteristic size of matter or antimatter region. But a consistent calc of separation and following annihilation

leads to a much smaller concentration of nucleons and antinucleons, disagreeing with present density of nucleons

Annihilation continues during radiation-dominated stage, but expected consequences of prolonged annihilation are not observed. Thus, even with account of phase separation, charge-symmetric theory does not agree with observations.

Consider therefore charge-asymmetric Universe with excess baryons always. Early, excess of baryons is small given number of pairs, so Omnes phase separation is plausible then

For $T = 300\text{MeV}$, charge asymmetry manifests itself only in at $T > 1\text{MeV}$, when there is an abundance of electrons and positrons and RR spectrum takes equilibrium form.

Finally, charge asymmetry leads to $n(\text{baryon today}) = n(\text{baryon charge density initially})$.

It would nevertheless be very interesting to find evidence now of hadron era phase separation.

Hagedorn theory that the number of charged particles is infinite is contradicted by experimental results of QED.

7. Kinetics of Elementary Particle Processes

In earliest stages of the hot Universe, neutrinos (+anti) are in thermo equilib with other particles. Creation of neutrinos mainly by $e^- + e^+ \gg \text{neutrino (+anti)}$ with relativistic cross section

$$\sigma \sim \frac{g^2 \times E^2}{h^4 \times c^4}, \quad (1)$$

where $g \sim 10^{-49}\text{ergscm}^3$ is the weak interaction constant

Given particle energy of kT , time to reach equilibrium $\tau = 1/(\sigma \times n \times c)$, and previous relation between universe time t and temperature T , we obtain dependent of τ and t :

$$\tau \sim \frac{[G^{5/4} \times h^{13/4}]}{[g^2 \times c^{1/4}]} \times t^{5/2} \quad (2)$$

(Landau & Lifschitz for statistical factors). When τ is greater than t , neutrinos no longer interact either with other particles or with one another. Equating them leads to $t \sim 0.1\text{s}$ without consideration of numerical factors but showing the dependencies of G and g . More accurate calculations follow, including consideration of μ neutrinos.

Present temperatures neutrinos compared to photons is then (Peebles)

$$T_{\text{neutrino}} = (4/11)^{(1/3)} \times T_{\text{photon}} \sim 0.7 \times 2.7\text{K} \sim 2\text{K} \quad (3)$$

But mass of neutrinos could be $\leq 100\text{eV}$, while background cosmic neutrinos would have energy $5 \times 10^{-4}\text{eV}$,

so observation of the background would require measurement improvement by 10^6 .

RR spectrum tells us about $z \sim 10^6$ at $t \sim 1\text{yr}$; neutrino spectrum could tell us about $z \sim 10^{10}$ at $t \sim 0.1\text{s}$!

Particles that decay spontaneously disappear exponentially as Universe expands. Stable particles would remain if annihilation reactions do not occur.

Y FIGURE 30 FOR TEMPERATURE-DEPENDENCE OF PARTICLE RELATIVE ENERGY DENSITY

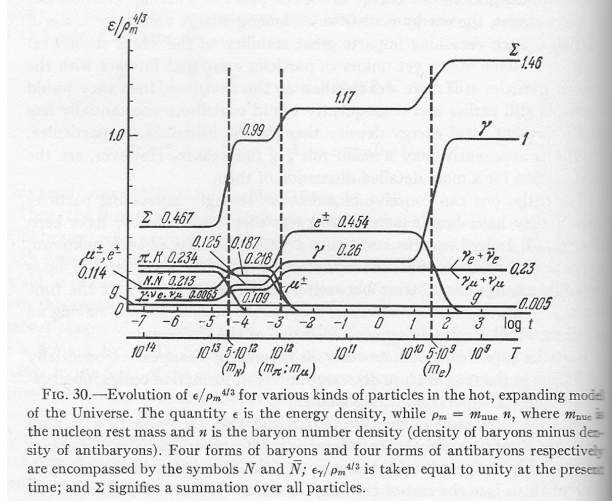


FIG. 30.—Evolution of $\epsilon/\rho_m^{4/3}$ for various kinds of particles in the hot, expanding model of the Universe. The quantity ϵ is the energy density, while $\rho_m = m_{\text{nue}} n$, where m_{nue} is the nucleon rest mass and n is the baryon number density (density of baryons minus density of antibaryons). Four forms of baryons and four forms of antibaryons respectively are encompassed by the symbols \bar{N} and \bar{N} ; $\epsilon_\gamma/\rho_m^{4/3}$ is taken equal to unity at the present time; and Σ signifies a summation over all particles.

?? MISSING TEXT FOR APRIL AND MAY RESULTING FROM IMAC FAILURE

MAY 12 SUMMARY

Introductory Remarks2

- Concerning Gravitation by MTW, a new edition (printing) was published in 2017 by Princeton University Press after the original in 1973 by Freeman. This new edition contains by David Kaiser describing the style of the original, the publishing history, and reactions to it. The new edition also contains an additional preface by MT that focuses on the status of the material in the text in light of developments subsequent to the original—chapter by chapter. Perturbations in the early Universe that could lead to structure formation are not addressed in MTW, though the papers by Lifschitz and Khalatnikov are cited (see point b).s
- The 1961 textbook by Landau and Lifschitz entitled the *The Classical Theory of Fields* does not contain material about GTR cosmology that goes beyond the simple Friedmann models, even though Lifschitz himself in 1946 and with Khalatnikov in 1964 addressed GTR perturbations.
- The 1972 monograph by Weinberg, *Gravitation and*

Cosmology: Principles and Applications of the GTR, does contain material about GTR cosmology that goes beyond the simple Friedmann models, in particular descriptions of the early hot Universe and perturbations that could lead to galaxy formation. There are citations to work by Z&N and to Lifschitz, among many, many others.

11: Instability in the Hot Model

Approach of last chapter here applied to RD period, when matter completely ionized, the radiation density dominates, and the matter is coupled to the radiation. For $\omega_0 = 1$, there is a short period, when the matter is still completely ionized, and the sound speed varies as $b = \frac{(c/\sqrt{3})}{\sqrt{[1+3\rho_m/4\rho_r]}}$. Matter and radiation densities become equal when $z = 10^4\omega_0$ or $t \sim 2 \times 10^{11} \times (\omega_0)^{-2}$ s.

????? During the period the Universe is filled with a medium whose equation of state is, $P = e/3 \sim a^{-4} \sim t^{-2}$, and sound speed is $b = c/\sqrt{3}$. A definite value for the temperature follows, while the matter density still requires specification of several parameters.

With the help of the Jeans criterion, let us find the conditions dividing regions of stability and instability.

Perturbations are of the form $\delta = \delta\kappa(t) \times \exp(k \cdot \mathbf{x} * i)$, where $k = k_0 a(t_0)^{-1}(1+z)$ and $\lambda = \lambda_0/(1+z)$. k_0 and λ_0 refer to the present. With the Jeans criterion taking the form $(b \times k)^2 = 4\pi G\rho$, and substituting values of b and ρ for the RD era, we obtain

$$k_{\text{Jeans}} = \frac{3}{(\sqrt{8} \times ct)} \quad (4)$$

and

$$\lambda_{\text{Jeans}} = 2\pi/k_{\text{Jeans}} = ct \times 4\pi \times \sqrt{2}/3 \quad (5)$$

The Jeans length is therefore of the order of the distance over which pressure gradients (sound waves) can equalize density.

The regions of stability and instability are conveniently seen in Figures 43 & 44. Also see Weinberg, Figure 15.6,

See slides PPT 36 & 38

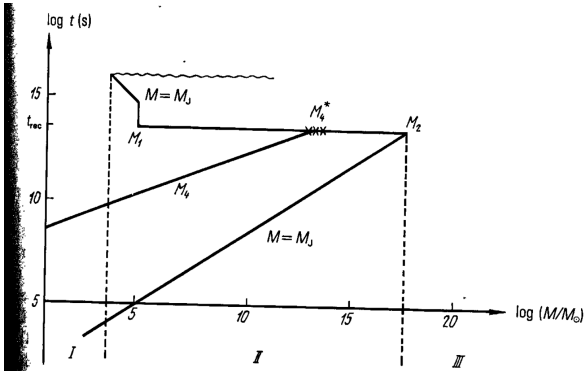


FIG. 43.—The regions of stability and instability on the $(\log t, \log M)$ -plane for $\Omega = 0.025$. The line $M = M_J$ separates the stability region from the instability region. The line $M = M_4$ is the boundary of the region in which the perturbations effectively dissipate (cf. § 2 of this chapter). Masses $M > M_J$ are located in the instability region, masses $M < M_J$ are located in the stability region, and masses $M < M_4$ exponentially decay with time. The time of recombination $t = t_{\text{rec}}$ coincides, for $\Omega = 0.025$, with the time when the matter density and the radiation density are equal. M_J is the Jeans mass after recombination; it decreases somewhat after $t \approx 10^{16}$ s (cf. § 8 of chap. 14). The wavy line denotes an arbitrarily chosen time when secondary heating of the matter begins (cf. chap. 15). The remaining details are discussed in the text of this section.

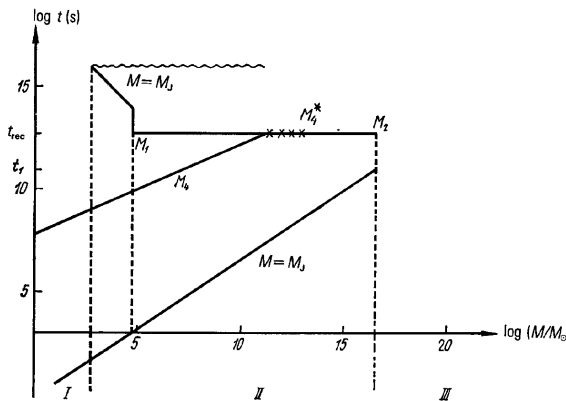


FIG. 44.—The regions of stability and instability in the $(\log t, \log M)$ -plane for $\Omega = 1$. The notation is the same as in Fig. 43. The matter density and radiation density are equal at the time $t = t_J$; and recombination takes place at the time $t_{\text{rec}} > t_J$. During the interval $t_J \leq t \leq t_{\text{rec}}$, the Jeans mass is constant.

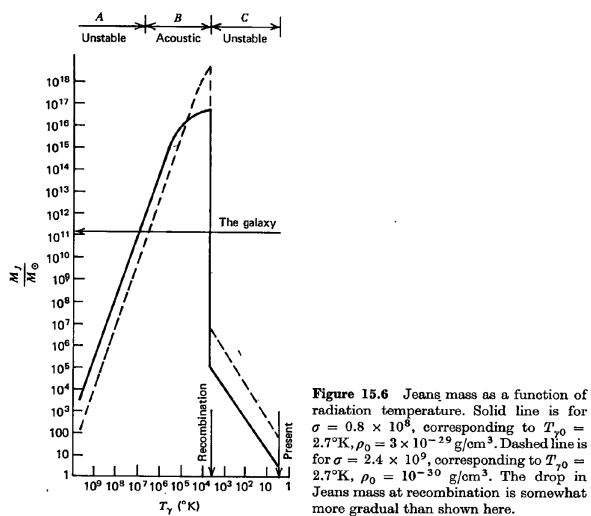


Figure 15.6 Jeans mass as a function of radiation temperature. Solid line is for $\sigma = 0.8 \times 10^8$, corresponding to $T_{r0} = 2.7^\circ\text{K}$, $\rho_0 = 3 \times 10^{-29} \text{ g/cm}^3$. Dashed line is for $\sigma = 2.4 \times 10^9$, corresponding to $T_{r0} = 2.7^\circ\text{K}$, $\rho_0 = 10^{-30} \text{ g/cm}^3$. The drop in Jeans mass at recombination is somewhat more gradual than shown here.

Other points in this chapter:

- as a result of dissipative processes, decay of a wave is determined by conditions during the last part of every period considered because the increase in photon MFP overpowers the increase in the wavelength;

b. conclusion that difficult-to-observe particles give rise to a rather small decrease in the amplitude of oscillations compared to neglecting them;

c. hypotheses that supermassive stars or globular clusters result from entropy perturbs;

d. conservation of vortex velocity upon early stages of expansion, matching perturbs when the eqn of state change; and

e. Sakharov oscillations

12: Gravitational Instability in the GTR

GTR approach necessary for perturbations with $\lambda \gtrsim ct$ in a fluid with eqn of state $P = e/3$.

Method is to take homogeneous, isotropic Friedmann model but then to replace metric g by $g_0 + h$, where h represents perturbations; analogously, stress-energy tensor changes from e to $e_0 + \delta e$, with δP determined by eqn of state, and finally perturbed velocities u are assumed small, with u_0 fixed via the identity $u \cdot u = 1$. These expressions are then substituted into GTR eqns, relating h , δe , and u , and yielding their time evolution once initial perturbations are specified.

See slides PPT 41 & 42 for the metric and the resulting eqns for the perturbs from the GTR eqns. All computations are done in the linear approx in which the quantities h are first-order. Then perturbed values of e , P and U occur only in second order.

Two caveats:

1. GTR eqns put some restrictions on these initial values.
2. Coordinate system choice allows apparent unphysical results; distinguishing between them is important.

Follow approach of Lifschitz and many others: synchronous reference system is used to study the perturbations, and their consequences are studied in other coord systems. Nonlinear approximations likely lead to important changes to be examined in later chapters.

So consider perturbations in spatial regions which may be large with respect to ct but small with respect to radius of curvature during the period studied; $a \gg ct$ during the early stages of evolution, conditions equivalent to perturbs in a flat model with ρ_{critical} . This will yield possible galactic evolution paths; Lifschitz studied more general cases.

Solutions of the eqns will be as plane waves of the form $Q = e^{i\kappa \cdot x}$ on the background of a spatially homogeneous and isotropic evolving Universe with the same invariances as the unperturbed solution, with κ a certain vector and Q a scalar.

Then tensors can be constructed from κ and Q . There will also be a vector $P = \kappa \times Q$, and still another vector $\Sigma = Es \times Q$, with Es perpendicular to κ .

These are scalars, vectors and tensors only in 3-d space.

The scalar Q will describe density perturbations and Es will describe velocity perturbations. Another tensor with a plane wave dependence will describe gravitational waves.

Scalar : The main term for very early times is that the fractional energy density varies linearly with time. For late times, the fractional energy density would vary as $\cos[(\kappa \times \eta)/\sqrt{3}]$, corresponding to acoustic oscillations with a speed of $c/\sqrt{3}$ and to constant-amplitude density perturbations. This exact result supports the results of the intuitive analysis. The exact theory also works with metric perturbations, which would be finite as t tends to zero. There was a line missing in the translation on page 292..

The independence of the metric perturbations with respect to time during early stages of the expansion accords completely with the idea underscored by the intuitive analysis of long-wave perturbations. This independence is also in accord with the independent evolution of different regions of the Universe with different initial conditions.

For $\lambda \ll ct$, the metric perturbations tend to zero and we are left with a description of sound waves. But this result applies to the eqn of state of a RD plasma, where $b = c/\sqrt{3}$, with the pressure gradient smoothing perturbations, so the “sound” horizon is important. For dust, $P = 0$, there is no sound propagation to smooth geometry and density perturbations. Density perturbations continue to grow for $\lambda < ct$, but metric perturbations remain constant.

One very important conclusion of Lifschitz's work that remains valid is that to explain finite perturbations today (galaxies!), it is sufficient for δ to tend to 0 as t tends to 0, whereas the metric perturb must remain nonzero as t tends to 0. Novikov found $h \sim 10^{-2}$ to 10^{-3} as t tends to 0, corresponding to galaxy clusters.

Vector (Rotational) perturbations case exhibits differences from Hubble expansion. The solutions show that metric perturbations grow as time approaches zero, leading to the conclusion that initial rotational perturbations are incompatible with a Friedmann model. This conclusion is important in any discussion of galaxy formation in the vortex theory.

Tensor perturbations have two independent polarizations for a given wave vector. If the wavelength is less than ct , the solution describes a wavelike gravitational field. So when the wavelength becomes less than the horizon size, usual energy density computations apply:

Amplitude $h \sim (1+z) \sim a^{-1}$, and energy density $e \sim (1+z)^4 \sim a^{-4}$. The wave velocity is c . The density and velocity perturbations are not connected with gravitational waves.

Matter (coming?) velocity relative to perturbed coordinates is zero in the field of a gravitational wave, but particle velocities do change, so a sphere becomes a time-varying ellipsoid in the directions perpendicular to the

velocity of the wave. If the wave passes through an ideal fluid, energy is not dissipated, so entropy does not grow and new waves are not created. Viscosity would change this

Entropy perturbations could arise as inhomogeneities in the eqn of state, with one approximate form being

$$P = e/3[1 - B(x)e^{-1/4}], \quad (6)$$

with consequent effects on the metric and motion. Initial entropy perturbations would give rise to adiabatic density perturbations, and, in particular, to growing-mode adiabatic perturbations if the wavelength is sufficiently large, though this is not a relativistic effect. Entropy perturbations corresponding to masses between one solar mass and 10^4 solar masses would only cause decaying RD plasma oscillations before recombination. For masses greater than 10^4 solar masses, the entropy irregularities are preserved. Such perturbations could be related to the formation and evaporation of PBHs, leading to entropy production, possibly all entropy!

One interesting idea is a quasi-isotropic solution with a uniform distribution of perturbations described by this metric:

$$ds^2 = (cdt)^2 - [t \times a(x) + t^2 b(x) + \dots] dx dx \quad (7)$$

The functions a and b are of the spatial-metric type, with 3×3 indices, and x is a spatial vector.

A general result is that Friedmann behavior near the singularity is compatible with density perturbations and gravitational waves, which may not be small, but not with vortex perturbations. Thus the quasi-isotropic solution, or entropy perturbations, represent cosmological solutions not in conflict with the present state of the Universe, deviating least from the strictly homogeneous solution,

Perturbations whose wavelength is comparable with the size of the Universe requires analysis with math beyond plane-wave theory. Assume ω unequal to unity to exclude the flat model. The ratio of the wavelength of the perturb to the radius of the model is constant during the expansion. Solutions are constructed similar to the methods for constructing spherical harmonics. Scalar functions are considered.

Some remarks about the possible periodic distribution of quasars as a function of redshift.

The concluding remark in this chapter is as follows:

ZN: "One indeed ought to expect that the spherical-wave method will find wide application in the theory of perturbations of the homogeneous, isotropic Universe in the very near future." N.B.: This is a prediction from 1975!

LF: See slide 43 interpreting the CMB Planck observations as a function of the spherical harmonic parameter l , a result from 2009 and later, as well as from WMAP from 2001 and later.

JUNE 15 SUMMARY

13: Statistical Theory

Any small perturbation can be represented as a linear combo of independent plane waves. Further steps are to examine wave interactions and to solve nonlinear problems.

Galaxy forms and locations are random, suggesting random initial perturbations and a statistical description of the Universe subject to the fundamental laws of physics.

An initial assumption of density perturbations in boxes fails because of interactions among neighboring boxes.

Consider instead a plane wave expansion of the density perturbations:

$$\Delta\rho = \sum_k (A_k \Psi_k(x)) \quad (8)$$

where $\Psi_k(x) = V^{-0.5} e^{(ik \cdot x)}$

(Deltarho = Sumk Ak * Psik(x) where Psik(x) = V**-0.5 * exp(i*k dot x))

The Ψ functions satisfy orthonormal conditions. A convenient dimensionless quantity is

$$\Delta k = [k^3 / (2\pi^2 * n)] * \sum_k (|A_k|)^2. \quad (9)$$

If for all k Δ is small, then the density perturb is small.

For a bounded volume $V = L^3$, then $kx = 2\pi nx/L$, etc., where the n values are whole numbers.

A reasonable definition of a random function is one whose Fourier coeffs are random, and the randomness is not resolved by the physical interaction while the perturb is small. The randomness hypothesis is connected with the idea that we can choose many different volumes in the Universe. Each has a definite density function and a single set of amplitudes A_k . How often is a given A_k value encountered? 1

Let $A_k = B_k + iC_k$ and consider over N volumes and respective k values the probability $P(B, C, \dots)$ for the appearance of given values of the Fourier coeffs. A natural form for this probability is proportional to

$$e^{(-B_k^2/[2*\beta_k^2])} * e^{(-C_k^2/[2*\gamma_k^2])} \quad (10)$$

At an early stage near the singularity, the integral which determines the Fourier coeffs reduces to a sum over causally disconnected regions (if there is no period “before the singularity”). Hence the assumption of a normal distribution for the A_k is natural.

Even for small inhomogeneities of 10-20%, the astronomer wants to know their form and amplitude, not

Fourier coeffs. While the average value of δ vanishes at each point of space, the average of its square does not. The properties of the Fourier series leads to

$$\langle \delta^2 \rangle = \sum_k \langle A_k^2 \rangle / V \quad (11)$$

With normal distributions for B_k and C_k , we then find for the prob that a given value of δ is obtained at any given point, with Δ the same for all points and independent of time,f

$$P(\delta) = [1 / (2 * \pi * \Delta)^{0.5}] * e^{(-\delta^2 / [2 * \Delta])} \quad (12)$$

Note well: δ and Δ represent different quantities; δ is the dimensionless density amplitude.

This function describes the amplitude of the inhomogeneities, but says nothing about their spatial structure

The correlation function $f(r)$ characterizes their spatial structure, with

$$f(r) = \frac{\langle [\delta_x * \delta_y] \rangle}{\langle \delta^2 \rangle} \quad (13)$$

and where $r = x - y$

This correlation function will be positive for small values of r , but its sign will vary for larger values. The natural conclusion is that the first zero of this function will define regions with the same sign of δ . For example, if $f(r)$ is given in terms of the spectral function β_k characterizing the amplitude of waves of various length and is concentrated in a narrow interval around a wave number k_0 , then the first zero is at $r_0 = \pi/k_0$, half a wavelength

When has a significant fraction of the mass passed into gravitationally bound objects? Suppose that the β_k with $k < k_{Jeans}$ grow with time as a consequence of gravitational instability. Fragmentation will have occurred when the growing Δ is of order unity.

A good and simple description of the matter inhomogeneity is given by average mass and its deviation through

$$\mu = \frac{\langle \delta M \rangle}{\langle M \rangle} = \frac{\sqrt{\langle M^2 \rangle - \langle M \rangle^2}}{\langle M \rangle} \quad (14)$$

Assume that all matter is distributed in the form of isolated bodies of mass M_1 with average density ρ_1 , so the number density of bodies is $\langle \rho \rangle / M_1$ and the volume of each body is $v = M_1 / \rho_1$. Then μ has the following behavior:

1. For $\langle M \rangle \gg M_1$, many bodies are found in the volume under consideration, so μ is small and tends to zero as $\langle M \rangle$ tends to infinity

2. If $(\langle \rho \rangle / \rho_1) * M_1 < \langle M \rangle < M_1$, then sometimes there is only one or not even one body in the volume under consideration and $\mu \sim \sqrt{M_1 / \langle M \rangle} > 1$. For $\langle M \rangle < \langle \rho \rangle * M_1 / \rho_1$, i.e., for $\langle M \rangle < \langle \rho \rangle * v$, the volume under consideration is less than that of a single body and

$$3. \mu \sim \sqrt{\rho_1 / \langle \rho \rangle} > 1$$

How does μ behave for $\langle M \rangle \gg M_1$, for objects containing many of the smaller bodies? Naively, much as does a statistically independent distribution distribution of particles. The average number of little bodies in such an object is $\langle N \rangle = \langle M \rangle / M_1$, while

$$\mu = \langle \delta N \rangle / \langle N \rangle = 1 / \sqrt{N} = \sqrt{M_1 / \langle M \rangle} < 1 \quad (15)$$

for $\langle M \rangle > M_1$

But this is not always correct. There is no universal description of the behavior of the function μ since it depends on the isolation process. Indeed, a study of the processes in large volumes containing many objects and leading to small μ values can give valuable info about the universe and its large-scale structure.

The law $\delta N = \sqrt{N}$ is only obtained given a random—not correlated—arrangement of discrete objects in space, corresponding to the hypothesis of a God who, from outside, sows space with galaxies and that they fall into regions independent of how the preceding ones are distributed. But this hypothesis is evidently unacceptable, since gravity from existing objects affects the growth of small perturbs. An evolutionary formulation is necessary from a uniform distribution. Seemingly perturbs grow from the inflow of matter from neighboring regions. But this reasoning is not valid in the case of gravitational instability, taking account of the long-range nature of gravity.

Considerations of Jeans theory allows one to say that the increase of matter at the center (in a spherical configuration) is not from neighboring regions, but from infinity! Thus there is not an anticorrelation among neighboring galaxies.

The final conclusion is that the fluctuation law $\delta N = f(N)$ for the distribution of discrete objects depends on the law for the original small perturbs. In principle, $\delta N \sim 1/N^{1/6}$ or $\delta N \sim N^{2/3}$ are possible, depending on the spectrum of small perturbs. Observational studies can give insight into the initial state.

Concerning limitations of the linear theory, the first is that it is practically difficult to calculate the properties of a surface of given δ for a distribution function whose Fourier expansion is specified. Second, there are conceptual problems in matching the topology of regions with particular δ values, as small islands say, with the topology of known astronomical objects.

The root of these difficulties is that astronomical objects result from strong nonlinearities, which are addressed in the next chapter.

14: Nonlinear Theory and Thermal Instability

Three ways to approach the nonlinear problem, possibly in combination:

1. Exact solution with special initial conditions;
2. Approximation method for extrapolating the linear solution to the general case; and
3. Qualitative explanation of the properties of the general exact solution.

Spherically symmetric perturbs can be analyzed exactly because the effect of neighboring perturbs vanishes. Second method takes account of the tidal action of neighboring perturbs, but this is an approx.

Analyses are only for dust, for which pressure vanishes. The simplest spherically symmetric case is of a sphere with perturbed density Ω' on a Friedmann background with Ω , where $\Omega' > \Omega$. With no extra mass, there is a hole in the shell outside the higher density region.

If $\Omega \leq 1$, then the two cases $\Omega' \leq 1$ and $\Omega' > 1$ are possible. In the first case, the perturbed sphere expands indefinitely and a bound object does not form. In the second the perturb behaves as a closed Friedmann model, going from expansion to contraction and eventual recollapse. In this “Swiss-cheese model”, the many such perturbs do not affect the average expansion. Differences occur if there is not initial symmetry or inhomogeneity. If there is pressure, then infinite density does not occur over the whole volume simultaneously, leading to shock waves and nonzero pressure and entropy.

In the early moments of the solution, when the unperturbed density is large and perturbations small, what critical perturb amplitude leads to the formation of gravitationally bound objects. The answer is

$$\Delta_{crit} = \frac{3}{5} \frac{1 - \Omega_0}{\Omega_0(1 + z)} \quad (16)$$

14.2

From observations in the expanding Universe, the amplitude of density perturbs become of order unity when the linear size of inhomogeneities is much less than the horizon ct and the radius of curvature a . Thus a linear perturb theory loses its validity when the use of Newtonian physics remains valid, i.e. when relativistic effects are insubstantial. Additionally, there are cases where gas pressure negligibly affects perturb growth, especially

adiabatic perturbs during the prerecombination era RD era. Below we consider post recombination effects of such perturbs.

Eulerian coords r of particles are written as functions of their Lagrangian coords s as

$$r = a(t)s + b(t)x(s), \quad (17)$$

where the first term corresponds to unperturbed motion. Neglecting the second term, we find

$$u = \frac{dr}{dt} = s \frac{da}{dt} = r \frac{1}{a} \frac{da}{dt}, \quad (18)$$

which is the Hubble expansion law. Thus the Lagrangian coords s are defined as the comoving cords of the unperturbed motion. The second term describes perturbs, exact for small, growing perturbs; we shall use it even for large density contrasts.

Earlier it was shown that in the linear approx and when $P = 0$, a perturb of any form grows, but its form remains unchanged:

$$\delta = \delta_0 \frac{r}{a} \phi_1(t) \quad (19)$$

and

$$w = w_0 \frac{r}{a} \phi_2(t) \quad (20)$$

But we also stipulate that, while the density distribution is arbitrary, the peculiar velocity w is vortex-free. A reformulation incorporating this condition is that w_0 is derivable from an arbitrary potential, $w_0 = \nabla\phi$; then $\nabla \times w_0 = 0$. We assume too that the $\delta_0 = -\nabla \cdot w_0$.

In the construction of the approx nonlinear theory, we select as an extrapol the linear formula $w = w_0(s) * \phi_2(t)$. The peculiar velocity is then

$$W = \frac{dr}{dt} - Hr = \frac{1}{a} \left(a \frac{db}{dt} - b \frac{da}{dt} \right) x \quad (21)$$

The Hubble parameter is $\frac{1}{a} \frac{da}{dt}$, $x(s)$ is vortex-free, and ϕ_2 and b are related. This variant of the linear approx is useful for the following qualitative reason. In the absence of other forces, the exact solution takes the form

$$r = a_0 ts + tv(s) + s \quad (22)$$

Then particle trajectories intersect and infinite density is achieved. Clearly the perturbs are large near this singularity. But in the general case, the sing. Takes the form of a 2D surface. Only for degenerate cases does the intersection occur along a line or at a point. Now take

into account grav. forces: near the 2D sing these forces are finite, so they do not exert a drastic influence on the perturb growth and do not seriously affect the general picture. Thus it is reasonable to seek a solution for large perturbs in a form valid for small perturbs and small gravitational forces. And it becomes easy to calculate other quantities such as the density and the velocity. For a given $r(s)$, the density equation in Lagrangian coords is exactly soluble.

In the linear approx, $b(t)$ is well known and density perturbs are proportional to the ratio $b(t)/a(t)$, also well known.

The density can be rewritten in this form:

$$\rho = \frac{\langle \rho \rangle}{[1 - (b/a)\alpha][1 - (b/a)\beta][1 - (b/a)\gamma]} \quad (23)$$

Here, α , β and γ are functions of s only, while b/a is a universal function of t (depending on ω_0 also), conveniently expressed in terms of z . The generally unequal functions α , β and γ depend on the specific form $x(s)$ of the initial perturb and thus characterize the deformation along the three orthogonal axes of the deformation tensor. For definiteness, choose $\alpha > \beta > \gamma$. V v

While the case $\alpha < 0$ is possible, if $\alpha > 0$, then $[\alpha(b/a)]$ grows and can reach unity in the course of the evolution. Then it follows from the density equation that the density becomes infinite there. This arises as a result of the 1D contraction along the axis related to α . The picture that results is that when the perturbs become sufficiently large, flat pancakes of collapsed dust form in various places.

This general picture is supported more generally. It is necessary to note that contraction along one coord can be accompanied by contraction or expansion in the plane of the pancake. Based on a complicated probability distribution function (pdf) for α , β and γ obtained by Doroshkevich [LF interpretation of the text; note too that this pdf is given in the text], only 8% of the matter contracts along all three axes, while 84% contracts in one direction but expands in one or two.

The value 8% is close to Oort's estimate of ~6% that matter is compressed in all three directions. It is however not evident that only this 8% eventually becomes gravitationally bound. [see Oort, J.H. 1958, in La structure et l'évolution de l'univers, 11 Conseil de Physique Solvay (Brussels: Stoops) and 1970, Astronomy. Ap., 7, 384].

Physical applications of this pancake picture will be discussed in the next chapter.

14.3

In nonlinear spectral theory, the approx solution for dust can be written as functions of spatial coords multiplied by functions of time.

Consider now the case where pressure is large, important for processes before recombination or small-scale entropy perturbs after recomb.

In the linear approx, the eqns for Fourier amplitudes satisfy second order, time dependent dif eqns so the amplitudes A_k are independent of one another, and the A_k can vanish.

In the nonlinear case, the eqns become

$$a \frac{d^2 A_k}{dt^2} + b \frac{dA_k}{dt} + c A_k = F(A_{k'}, A_{k''}) \quad (24)$$

thus harmonics of the original spectrum can arise and $A_k = 0$ initially can change to $A_k > 0$ or $A_k < 0$ subsequently given a nonzero function F . Higher order approxs are possible, but we shall not consider them.

The function F will describe an interaction yielding a new wave vector $k = k' + k''$. Basic physical results of the nonlinear interactions are as follows:

1. Neglecting viscosity, interacting longitudinal waves will not lead to the emergence of transverse waves. Consequently, in the quadratic (second-order) approx, vortex-free motion only gives rise to vortex-free longitudinal waves.
2. Since the interaction of transverse waves gives rise to longitudinal waves, density perturbs can arise in the second order—as well as for higher orders. Therefore the amplitude of short-wave acoustic density perturbs generated is of order $\delta \sim (u/b)^2$, where u is the amplitude of the transverse motion. Given vortex (turbulent) motions in the prerecombination RD plasma, this turbulence leads to large density perturbs after recombination, when radiation pressure ceases to act on the matter.
3. The interaction of short-wavelength ($\lambda < \lambda_0$) longitudinal perturbs leads to long-wavelength longitudinal perturbs (including growing density perturbs). If the initial spectrum falls sufficiently steeply on the long-wave side, then this process is the most important source of density fluctuations on large scales. Under reasonable assumptions the newly created (by the nonlinearity) long waves satisfy $A_k \sim k^2$, leading to

$$\frac{\delta_M}{M} \sim \sqrt{(Ak^2 \times k^3)} \sim k^{7/2} \sim M^{-7/6} \quad (25)$$

This is explained below, but is evidently the extreme case of a huge number of short-wave perturbs combined with the initial absence of long wavelength perturbs.

4. Longitudinal waves with a wavelength $\lambda > \lambda_0$ for some λ_0 generate short waves by the nonlinear interaction, important for cosmology. In accord with the linear theory, viscosity suppresses

long-wave perturbs corresponding to masses $M < M_J \sim 10^{12} M_\odot$. However, continuous generation maintains the perturbs in this wavelength interval. Shock waves may arise from these short waves. The emergence of a shock wave leads to entropy growth, whose fluctuations remain even after the longitudinal acoustic waves decay.

Nonlinear wave interaction theory is currently incomplete. But here are some properties of the general theory.

In an equilibrium situation, statistical mechanics says that each degree of freedom has the same energy θ ; then $A_k \sim \theta^{1/2}$, must be a solution to the kinetic eqn corresponding to $dA_k/dt = 0$ on the left-hand side (LF—the kinetic eqn?).

The equilibrium laws do not depend on the specific interaction mechanism. Creation of waves $k = k' + k''$ must be accompanied by the reverse, keeping the A_k at their equilibrium values. The theories of turbulence and fluctuations are always concerned with nonequilib situations with amplitudes in a small part of phase volume (values of k much smaller than the inverse interatomic distance) much higher than thermal motion amplitudes. Therefore we are usually concerned with a stationary but nonequilib situation.

In diffusion eg, with turbulence or fluctuations, there is ordinarily a flow of energy to the short-wave side, where the energy transforms into heat. In situations where $A_k \rightarrow 0$ as $k \rightarrow 0$ in part of phase space, a flow of energy in the reverse direction is possible. Keep in mind that equilibrium is characterized by $\langle A_k \rangle$, which is quite appropriate because the phase of the A_k is random and the distribution of the $|A_k|$ is Gaussian.

But these assumptions do not always apply to the spectral distributions under consideration here. For “pancakes” there is a density distribution with a large amplitude for short waves, which are not random. They are correlated with the long waves, all of which together form the flat pancake! Consequently, in problems concerning the emergence of pancakes and problems concerning shock waves, the spectral approach is worse than the direct approach of analysis in spatial coords.

14.4

Consider the question of the formation of large-scale clusters from discrete objects. There are two possible causes. The first is the presence of small perturbs of large linear dimensions in the initial perturb spectrum, which grow via gravitational instability. When their non-dimensional amplitude reaches unity, the matter has become clustered on the large scale. The second is due to nonlinear effects, which give birth to long-wave perturbs from short-wave ones.

Let the part of the spectrum of interest have an amplitude δ_M that is a “not too fast” decreasing function of M . In this case small units, discrete gravitationally bound bodies—are formed first but distributed in space nonuniformly due to the presence of weaker perturbs on larger scales.

Formation of larger units depends on the initial spectrum, independent in the first approx of the smaller scale. The growth of perturbs of $10^{15} M_\odot$ is the same for a gas of H atoms as for a gas whose elementary units are star clusters with mass of $10^5 M_\odot$. Assume the density perturbs at recombination satisfy

$$\delta_{rec} = \delta_\rho / \rho = b_0 \times M^{-\nu} \quad (26)$$

for $M > M_1$; and zero for smaller M .

For the growth law with $\Omega_0 = 1$,

$$\delta = \delta_{rec} \times [(1 + z_{rec}) / (1 + z)] = \delta_{rec} \times (t/t_{rec})^{2/3}. \quad (27)$$

Formation of discrete gravitational bound bodies will be when $\delta(M, z) = 1$, so the first appearance of bodies with mass M_1 occurs at time t_1 or z_1 given by

$$\Delta = b_0 \times M_1^{-\nu} \times [z_{rec} / (1 + z_1)] = 1, \quad (28)$$

yielding

$$z_1 + 1 = z_{rec} \times b_0 \times M_1^{-\nu} \quad (29)$$

The growth of mass occurs via the unification of smaller masses M_1 into a discrete bound aggregate with mass M , but this does not change the law

$$M(z) = M_1 \times [(1 + z_1) / (1 + z)]^{1/\nu} \quad (30)$$

Consider the case of an upper spectrum cutoff $\delta = 0$ for $M > M_2$. The short wave perturbs with $k > k_2$ (corresponding to M_2) in the process of growth are producing long-wave perturbs by nonlinear interaction. The Fourier amplitude of these new modes is $A_k \sim k^2$. The corresponding density perturbs in a volume containing a large average mass M , much greater than M_1 , is given by

$$\delta(M) = (A_k^2 \times k^3)^{1/2} \sim M^{-7/6} \quad (31)$$

for $k = M^{-1/3}$

By dimensional considerations, we obtain from $\delta(M_1) = 1$ at $t = t_1$ the coefficient in this formula, leading to the final conclusion for the growth with time of bound masses in the expanding Universe:

$$M = M_1 \times (t/t_1)^{4/7} = M_1 [(1 + z_1) / (1 + z)]^{6/7} \quad (32)$$

This law must be called a “self-similar clustering law” for every sufficiently steep initial spectrum (with $\nu > 7/6$) for the case of absent or very weak long-wave perturbs. The $\nu = 7/6$, $M \sim t^{4/7}$ law corresponds to the clustering of great masses, causally dependent by nonlinear effects on the early formation of small masses M_1 . These considerations are especially important in the analysis of entropy perturbs, where the natural assumption is that the smallest units M_1 are of the order of the Jeans mass after recomb, of order 10^5 or $10^6 M_\odot$ if the H temperature is equal to the RR temp.

Another case depends on a random (“white-noise”) initial fluctuation spectrum with $\delta \sim M^{-5}$ and $\nu = .5$; though the white noise spectrum has no foundation in cosmology, it leads to a growth law $M \sim t^{4/3} \sim (1+z)^{-2}$ and $M_{max} \sim 10^{12} M_\odot$.

The simple clustering theory operates with the average bound mass only.

Thermal instability could lead to a separation of a homogeneous gas into phases, namely dense cold clouds and low-density hot gas between them. Though unrelated to gravity, its effectiveness decreases for long waves. Therefore it is characterized by an optimal scale size. This is not the mechanism for separation of the cosmological plasma into discrete bodies, but could be important for galactic situations such as the formation of stars.

15: Theories of Galaxy Formation

15.1 Introduction

Several theories for galaxy formation in the hot model are in competition. But common are the assumptions that in the RD period (before recombination) the plasma is almost homogeneous and that the present-day structure arises after recombination ($z < 1400$). First, we shall discuss briefly four explanations for the deviations from homogeneity. (I shall not repeat historical notes given by Z&N—LF),

First, adiabatic perturbs are defined by the property that the ratio of numbers of baryons to photons is constant. In the period when radiation is predominant, adiabatic density perturbs represent acoustic oscillations for $M \lesssim 10^{17} M_\odot$. After recomb, the perturbs grow in accord with the law governing gravitational instability. Taking account of photon viscosity and damping of acoustic oscillations leads to a characteristic perturb mass of $10^{13} M_\odot$, close to the observed mass of galaxy clusters. During the nonlinear stage of growth, disks (pancakes) arise and the gas is heated by shock waves. The great diversity of gas states allows explanations for such various objects as quasars and elliptical and spiral galaxies. There is a possible explanation for galactic rotation and magnetic field. Adiabatic perturbation theory uses rather small initial metric perturbs — 10^{-3} to 10^{-4} in

dimensionless units — of the ideal cosmological model to obtain presently observed structure.

Second, perturbations of fluctuations in the ratio of baryons to photons are termed entropy fluctuations. In this model, the metric and the expansion dynamics do not “feel” any perturbations during universe evolution when radiation is predominant. Immediately after recomb., the neutral gas with $T \sim 4000K$ is not homogeneous. This temperature and the average density determine the Jeans mass $M_J \sim 5 \times 10^4 \times \Omega_0^{-5} \times M_\odot$. Large scale perturbations grow scale independently if $M \gg M_J$, while smaller scale perturbations do not grow at all.

A falling initial mass spectrum for perturbations is most probable. Then objects with the least mass consistent with the Jeans threshold form first, this minimum mass being $\gtrsim 5 \times 10^4 \Omega_0^{-5} \times M_\odot$; in other words, gas pressure limits this mass from below. Assuming instead that pressure is substantial leads to the formation of spherical bodies, not pancakes. We have tried to obtain the entire Universe structure from such entropy perturbations. Another tack suggested that objects with a mass of order $10^5 - 10^6$ transform into globular clusters, their unusual similarity previously unexplained. To explain the entire Universe structure, one could set the initial spectrum of entropy perturbations “by hand” so that the amplitude at about $10^{13} \times M_\odot$ is just that required to obtain at present $\delta_M/M \sim 1$. Then the results are roughly the same as obtained for adiabatic perturbations.

Third is the hypothesis of a charge-symmetric Universe, with annihilation where particles and antiparticles intermingle. However, the resulting gamma rays — from $p + \bar{p} \rightarrow \pi_0 + \text{other particles}$, and then $\pi_0 \rightarrow 2\gamma$ — have not been observed in the interval between 50 and 200 MeV. There are other arguments against this hypothesis, which has several variants.

Purely in theoretical grounds based on charge symmetry, a symmetry that CP violation shows is not exact, there is no reason to choose a charge-symmetric initial state of the Universe or a charge asymmetric initial state.

One aspect of charge symmetry is connected with entropy fluctuations. Until we examine a plasma with photons and baryons, it is natural to assume that the baryon density varies while the photon density is uniform. When we consider times $t < 10^{-6} \text{ s}$, when $kT \geq \text{mass} \times c^2$, and there are many baryons and anti baryons and as many photons, $n_B/n_{\bar{B}} = 1.00000001$ on average and appearances change. It is necessary to adopt this initial ratio ($n_B - n_{\bar{B}} \sim 10^{-8} n_B$) because those baryons present today are the survivors of the annihilation when the temperature decreased below $\sim \text{mass} \times c^2$. Undoubtedly the early stage of the hot Universe is quasi-charge-symmetric! But there must be a baryon excess and moreover, in the theory of entropy fluctuations this excess is not spatially uniform!

These fluctuations are very large compared with “statistical” fluctuations of order N^{-5} . Indeed, $M = 10^6 \times$

M_\odot corresponds to 10^{63} baryons, so $N^{-5} \sim 3 \times 10^{-32}$. But in the hot Universe with entropy we use $\delta_{n_B}/n_B \sim 10^{-10}$ before annihilation and $\sim 10^{-2}$ after annihilation. Although these numbers are very different, both are much greater than 10^{-32} . Although the fluctuations are not “statistical”, one can suppose that the smaller the scale, the larger the fluctuations. Then the assumption is not excluded that on some scale the fluctuations lead to an average baryon surplus of 10^{-8} . This leads to $0.99999997 < n_B/n_{\bar{B}} < 1.00000005$. This means that at the conclusion of the annihilation process, there are regions of matter and antimatter in which $n_B/n_\gamma \sim 5 \times 10^{-8}$ and $n_{\bar{B}}/\gamma \sim 3 \times 10^{-8}$ respectively. Thus the entropy-fluctuation hypothesis is naturally linked with the hypothesis of charge symmetry.

Fourth is the vortex theory, whereby the plasma of protons, electrons and photons is in turbulent motion superposed on the general expansion. The velocity of this motion is of order $(0.05 - 0.1) \times c$ and the maximum scale of the motion is much less than the horizon at recombination. The turbulent theory predicts a definite spectrum for the motion and a condition connects the scale, velocity and time to establish the motion. One parameter, e.g. the maximum scale L for the correlation, fixes the entire picture. It is also presumed that turbulence is subsonic during the RD state, so radiation pressure prevents density deviating from the average.

An estimate of the pressure and density fluctuations follows from oppositely moving fluid volumes creating a pressure difference of order $\delta_P = \rho \times u^2$, small compared to $P = \rho \times b^2$, with b the sound speed and u the fluid speed. Correspondingly,

$$\delta_P/p \sim \delta_\rho/\rho \sim u^2/b^2 \ll 1. \quad (33)$$

A spreading out and breaking down of the flow thus occurs, so the motion hardly differs from that of an incompressible fluid. When recombination ensues, the pressure cuts off and the sound velocity goes to zero. The motion then continues in accord with its inertia. But the incompressibility is not preserved and collisions between gas clouds disturb the inertial motion. The clouds first heat because of compression and shock waves, but later they cool. Gravity then begins to act and regions of increased density transform into bound objects when $z \sim 130$ (in contrast to $z \sim 5$ in the adiabatic theory).

The most important feature of the vortex theory, the rotation of the galaxies and clusters is thus inherited from the initial vortex motion of the plasma before recombination. One difficulty is that it is incompatible with small perturbations to the Friedmann model. Another is the difficulty of reconciling the turbulence theory with RR observations with respect to this parameter (which I understand to mean the aforementioned red shift events—LF).

15.2 Begin here after July 20, presumably on August 24.2

Now considered is the evolution of perturbs after recombination ($z \lesssim 1400$), carried to the stage of formation of gravitationally bound isolated masses. Limit the analysis to perturbs arising from initially adiabatic perturbs. Five properties are important:

1. The motion is derivable from a potential, so the vorticity is and remains zero, until a shock wave is formed;
2. The initial perturbs are small at recomb, so that afterward the perturbs remain small and linear theory is valid for a prolonged period;
3. Linear theory is applicable before recombination and at an early stage the perturb amplitude is an approximately smooth function of wavelength; The wavelength interval for galaxy formation is not wide, with a power law applying for the amplitude:

$$A_k \sim k^r. \text{ and } \sqrt{\delta_M} \sim M^{-\nu} \quad (34)$$

$\sqrt{\delta_M}$ was introduced earlier so that the exponents r and ν are related by $\nu = 1/2 + 1/3 \times r$. Damping is also important and depends on a parameter $M_0 \sim 10^{13} * M_\odot$. Its meaning is that perturbs decay for scales corresponding to masses $M < M_0$ and they do not for masses $M > M_0$.

4. After recombination, a restructuring of the motion takes place whereby growing perturbs develop that have an amplitude

$$\sqrt{\delta_M} = M^{-n} \times e^{-(M_0/M)^{1/3}} \quad (35)$$

with $n = \nu + 1/3$

The formulae presented here are valid for scales such that the perturbs become acoustic waves before recombination, ie for $M < 10^{17} * M_\odot$. The distinction between n and ν relates to the proportionality between δ_ρ and $u \times t/l$ for a growing mode in the postrecomb era.

5. After recombination one can neglect the pressure of the neutral gas when studying perturb evolution. The basis for this is that $M_0 \gg M_J$, where M_J is the Jeans mass for the neutral gas. As a result, the approx theory for the the growth of perturbs in dust is applicable.

By virtue of the first and fifth points, according to the approx theory, regions of infinite density arise. The nearest gas particles encounter the dense region and are stopped. We will therefore examine the motion of the gas, its heating by shock waves, and the subsequent fate of the compressed gas.

15.3 Shock Waves

{Math for shock wave description mostly too confusing for now—LF}

From a previous consideration of the approximate solution, infinite density occurs when this condition is met: $\alpha(q) \times (b/a) = 1$. This leads to a contraction of an ellipsoid (q is a vector) in one dimension to a flat figure — an ellipse aka pancake with infinite density. The mass of the ellipsoid grows in proportion to $(t - t_c)^{1.5}$, where t_c is the time when the density becomes infinite in the plane $qx = 0$ and $x = 0$. For a one-dim model with a single sinusoidal wave and with $\omega_0 = 1$, the density will be

$$\rho = \langle \rho \rangle \times [1 - \kappa \times (b_0/a_0) \times t^{2/3} \times \cos(\kappa \times qx)]^{-1}, \quad (36)$$

$$\text{with } \langle \rho \rangle = 1/(6\pi G t^2).$$

Now define $\mu = \kappa \times qx/\pi$, a type of Lagrangian coord, which is the ratio of the mass included between the origin $qx = 0$ and a given qx to the total mass in half of a period cell.

In the general case, the amount of matter at each point of the pancakes surface grows as $\sqrt{t - t_{c'}}$, with different values of $t_{c'}$ at different points in the plane of the pancake, whose surface grows as $(t - t_{c'})$.

It is particularly necessary to notice what matter is subjected to shock compression. It is the matter which does not manage to achieve infinite density as the nearby layers approach and also the matter which is expanding. For $t \ll t_c$ (during the linear stage) half of the matter contracts and half expands. See Table I.

TABLE I. Characteristics of Shock-Wave Compression

t/t_c	z/z_c	μ
1.0	1.0	0.0
1.025	0.983	0.1
1.33	0.83	0.333
1.96	0.64	0.5
6.1	0.30	0.76
28	0.1	0.9
Infinity	0.0	1.0

A computation gives, conveniently in terms of μ as the independent variable, the speed u at which the shock wave strikes the matter and the matter density in front of the shock wave ρ . Characteristic is the behavior for small values of μ , equivalent to small values of $t - t_c$ or $z_c - z$:

$$u \sim \mu \sim (t - t_c)^{.5} \sim (z_c - z)^{.5} \quad (37)$$

and

$$\rho \sim \mu^{-2} \sim 1/(t - t_c) \sim 1/(z - z_c) \quad (38)$$

and P approximately constant.

Consider the opposite limit, the complete absence of heat losses and transfer. Complete computations require numerical methods, but the asymptotic behavior at the beginning of the contraction, when $\mu \ll 1$, can be found simply. The pressure has a definite limiting value, larger than the first case by $11/9 = 1.22$, in the same limit, the amount of matter compressed by a hot shock is $(11/9)^5 = 1.1$ times larger than the amount of matter compressed by the shock with instantaneous cooling of the gas. This is because in the hot case the shock propagates from the plane $x = 0$ toward the infalling matter.

The average density of the compressed matter is 12 times larger than the matter density in front of the shock before compression, i.e., three times greater than immediately after the shock. Figure 46 shows the density distribution at t_c , when $\rho = \text{infinity}$ is achieved in the plane $x = 0$. Figure 47 gives the distribution at time $t = (7/6) \times t_c$, when about $1/4$ of the matter is compressed. Figure 47 applies to rapid cooling, and Figure 48 to the adiabatic case. 1 h

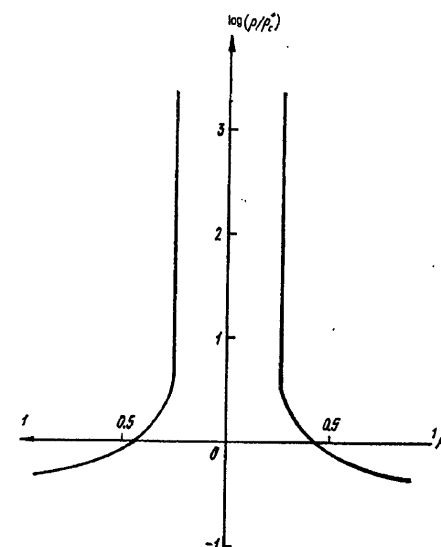
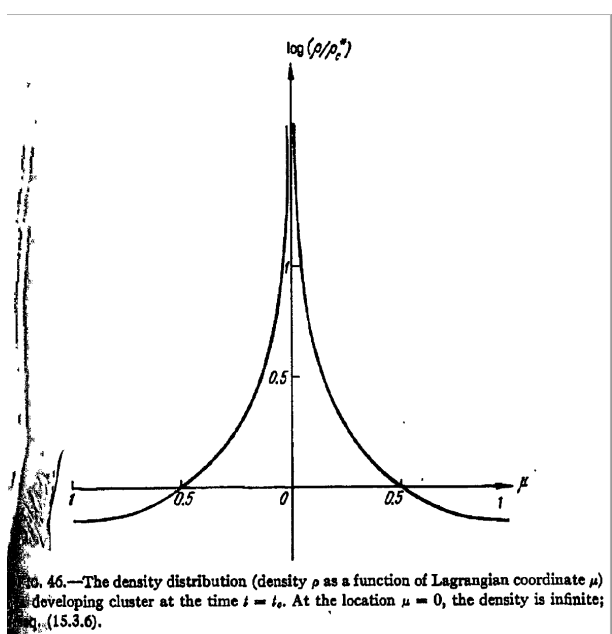


FIG. 47.—The same as Fig. 46, but after rapid cooling—at $t = 7t_c/6$, when the shock wave has just reached the Lagrangian coordinate $\mu = 0.25$. In Eulerian coordinates the region $\rho = \infty$ is compressed into a single point.

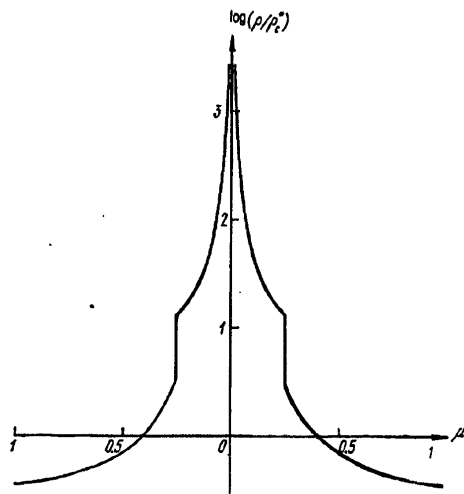


FIG. 48.—The same as Fig. 46, but for adiabatic compression. In this case, with cooling absent, the density does not become infinite after the compression.

NOTES BEGINNING AUGUST 30

From these formulae, when 10% of the matter is compressed by the shock ($\mu = 0.1$), this matter occupies a fraction $\alpha = 3 \times 10^{-4}$ of the volume, so its density is 300 times greater than the average. If instead 30% of the matter is compressed, $\alpha = 10^{-2}$ and the density is 30 times the average. The calculation has assumed strict adiabatic behavior, hence without heat loss. The true value of α for a given perturb type can only be smaller and the true density larger than the values presented.

In the future of the process, a mutual attraction among the compressed matter layers switches on, leading to a gravitational pressure. Numerical calcs show that when $t \sim 4t_c$, the process dies away. The compressed matter

is held in place by gravity, the falling of matter is suspended, and the shock weakens. An unrealistically large time would be needed for the shock to compress even 90% of the matter. Meanwhile, the new processes of radiation, star birth, etc are beginning, and this schematic picture of a one-dimensional adiabatic compression does not account for them.

15.4 Thermal Processes in the Compressed Gas

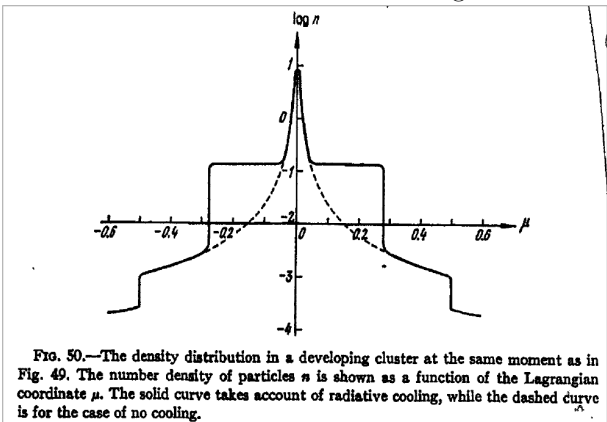
In the adiabatic approximation, the temperature of the gas compressed by the shock front is

$$T = 2.5 \times 10^6 \times z_c \times \mu^2 \times [M/(10^{13} \times M_\odot)]^{2/3} \quad (39)$$

for asymptotically small μ , for a sinusoidal wave, for zero initial temperature, and in the absence of heat losses and transfer. Now renounce the simplifying assumptions describing the temperature distribution and the thermal processes. But start from the pressure in the adiabatic picture. In the unperturbed gas, the compression leads to a finite density and a finite temperature.

Examining the processes in a homogeneous universe, we found that thermal exchange between matter and radiation ceases when $z \sim 200$, $T = 540K$, and $\rho \sim 0.8 \times 10^{-22} g/cm^3$ for $\Omega_0 = 1$. Subsequently, the pressure, temperature and density are connected by the adiabats (isentropic curves) of a monatomic gas, so $\rho \sim P^{3/5}$ and $T \sim P^{2/5}$. Thus, when $z + 1 = 5$, $T = 0.34K$ for the unperturbed gas (when the radiation temperature is 14 K). Upon compression to $P = 1.44 \times 10^{12} dyn/cm^2$, corresponding to the pressure in a pancake if mass $M = 10^{13} M_\odot$, we obtain $T = 400 K$ and $\rho = 0.5 \times 10^{-22} g/cm^3$, compared to the average matter density then of $\rho \sim 10^{-27} g/cm^3$. We thus obtain the thickness of an adiabatically compressed layer.

Heat losses are computed next, but I shall only summarize the results. Figure 50 shows the density distribution. The temperature distribution exhibits the opposite behavior in the sense of a reflection through the mu axis.



1. About 1% of the matter is subject only to adiabatic compression and has a very low temperature.
2. About 2-3% of the matter is shock heated to $10^2 K - 10^4 K$. It is not ionized and cools slowly through adiabatic expansion.
3. About 20% of the matter is shock compressed to $T > 10^4 K$. Then it cools to $10^4 K$ by radiating, and to a large degree, recombines.
4. About 25% of the matter is shock heated to $T > 5 \times 10^5 K$ up to $\sim 1.5 \times 10^6 K$ and remains hot.
5. Half of the matter is not subject to the shock action.

Indeed, it is observationally known that neutral H is practically absent between clusters. Convincing proof follows from quasar spectra with $z > 2$. Neutral H would totally absorb shortward of the Lyman-alpha line, but this radiation falls in the spectrum accessible to ground telescopes. Independent of the detailed pancake theory, it is inconceivable that there is no matter between galaxies, so it must be completely ionized. A suitable explanation for this ionization is one of the main problems facing cosmological theory.

Possibly the ionization is accomplished by the earlier quasars with $z > \sim 4$, not yet observable directly {SUPERSEDED?—LF}. Perhaps young bright galaxies are important. In both cases the radiation comes from the first pancakes. In any event, the calculational results depend significantly on the fundamental cosmological parameters, the Hubble constant and the matter density.

Furthermore, the hot compressed gas clouds — “pancakes” — cannot be observed directly as protoclusters in optical and ultraviolet against the background of other nearby sources. X-rays might be observable from the statistically rare largest clusters.

Finally, it is apparently possible to observe protoclusters via 21 cm radiation from the neutral H in the pancake region where the temp is too small for ionization to occur. The redshift of the line and the radiation’s association with a “pancake” would suggest the pancake’s epoch. The observational difficulty is related to the lack of knowledge of the absolute wavelength, unknown now because of the unknown redshift value at which the compressed gas was formed.

15.5 Cluster Masses and Protocluster Fragmentation

One ought to expect a distribution of masses for protoclusters and dependence on the form of the perturbation spectrum, i.e., the amplitude change versus wavelength. The mass distribution will be considered here, as well as the fate of the isolated gas bodies (protoclusters) already described. The gravitational instability of the

protoclusters leads to further fragmentation into galaxies and quasars.

To determine the time when nonlinear effects become substantial in a significant fraction of the matter, i.e. when a significant part is compressed into pancakes, it is enough in the first approx to find the fraction of the matter satisfying $\alpha \times b/a > 1$. The one-dimensional hydro calcs showed that the amount of matter shock compressed exceeds the amount of matter that, by itself satisfying the same condition in the absence of the shock, approaches infinite density. By integrating over the distribution function, one can find the fraction of the matter compressed as a function of time, which appears in Figure 51. In the figure, t_c is the time when $(\delta_\rho/\rho)^2 = 1$ as calced via linear theory. The dashed curve for cold clouds is distinguished from the solid curve primarily by the statistical nature, not by the one-dimensional nature.

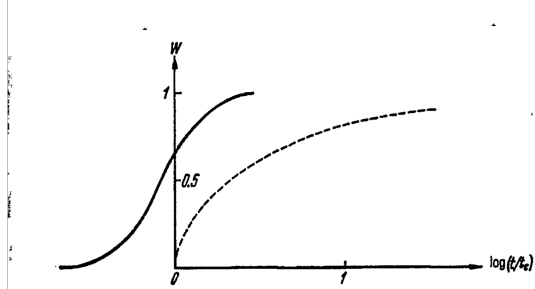


FIG. 51.—The time evolution of the fraction of the matter compressed by the shock wave. The solid curve is the result of the statistical theory, while the dashed curve is for a one-dimensional problem with a sinusoidal perturbation.

More detailed calls show that the thickness of the typical pancake (in Lagrangian coords) is of order R_c , while the area is $\sim 30R_c^2$.

Consider the fragmentation of a protocluster. The peculiarity of the problem is in examining the gravitational instability of a thin layer of matter with a thickness many times less than its longitudinal size. Also, the dense, cold matter is subject to the external pressure of the surrounding hot matter, with much lower density. During the initial pancake growth, this external pressure is greater than the gravitational forces within the dense layer. Though the general problem of a thin disk has been much studied, the problem here is simpler because there is no rotation and no peculiar velocities in the disk plane.

For a homogeneous disk with given surface density sigma (in g/cm^2), assume

$$\delta_\sigma/\sigma \sim e^{(w \times t + ik \times x)}, \quad (40)$$

with k and x two-dimensional, while the gravitational potential outside the disk is three-dimensional and satisfies the Poisson equation in empty space. Thus the solution requires a suitable boundary condition at the disk.

Accounting for the nonzero thickness of the disk and the pressure, we obtain

$$w = [2\pi \times G \times \sigma \times \text{abs}(k) - P \times h \times k^2/\sigma]^{1/2} \quad (41)$$

Thus, for a disk of nonzero thickness, there is a critical wavelength analogous to the Jeans wavelength for the 3-dimensional problem:

$$w = 0 \text{ at } k = k_j = 2\pi \times G \times \sigma^2 / (P \times h); \text{ and } \lambda = 2\pi/k_j.$$

There is also an important quantity not analogous to anything in the 3-d problem. This is the wave vector k_m and the wavelength λ of the most “dangerous” (most rapidly growing) perturb, for which w is a maximum. It satisfies $k_m = k_j/2$ and $\lambda_m = 2 \times \lambda$. If the pressure in the layer is determined only by the weight through gravity of the matter in the layer, then $P_c = \pi \times G \times \sigma^2/2$ in the middle of the layer; at the edges, $P_c = 0$. The average pressure is of order $G \times \sigma^2$. With $\sigma = h \times \text{avg}(\rho)$, this leads to

$$\lambda_J = h, \lambda_m = 2 \times h, \text{ and } \omega = 0.885 \times [4\pi \times G \times \text{avg}(\rho)]^{1/2}$$

An application of this theory is to the disintegration of a planar protocluster — a pancake — as just described. The inner, most dense (adiabatically compressed) layer must disintegrate into masses of $\sim 10^7 - 10^8 M_\odot$. A layer that cools to $10^4 K$ disintegrates into masses $\sim 10^{11} - 10^{12} M_\odot$. These latter masses are naturally identified with galaxies.

A hot gas with $T > 4 \times 10^5 K$ remains gravitationally unbound in part and in part forms a hot halo around masses of $10^{11} - 10^{12} M_\odot$, leading to a hypothesis that the most dense but small masses represent quasars and galactic nuclei.

With an initial density of 30 atoms / cm^3 , the average density can grow with adiabatic compression. After the formation of the first pancakes, the part of the gas enveloped by the shock wave is heated to a high temperature. The hard radiation from these layers then heats the gas to at least $\sim 10^3 K$, but this does not affect the general picture of the pancakes’ evolution. For pancakes formed later, the middle cold layer is then not so dense and cold as was the case for the first pancakes. One might then assume that the formation of quasars (and galactic nuclei?) ceases earlier than does the formation of galaxies. Possibly the sharp fall in the number of quasars and radio sources for $z > 3$ or 4 is related to this circumstance.

In the first pancakes, about 1% of the matter passes, by assumption, into quasars and galactic nuclei. This agrees with rough estimates derived from the assumption that the active life of quasars and quasi-stellar radio-quiet objects extends over $10^5 - 10^6$ years.

In every pancake with a dense layer, one can expect the formation of about 100 dense objects. In such a case, must the quasars be arranged in groups? Observations do not suggest this {STILL THE CASE?—LF}, and it should not be so. This follows if one keeps in mind that

the quasar active period is $10^5 - 10^6$ yr, many times less than the 10^{10} yr cosmological age and the formation time of the pancakes ($3 \times 10^8 - 10^9$ yr). At each time we observe $\sim 10^{-3}$ of the total dense objects — potential quasars — so that the average number of observed quasars for each protocluster is $\ll 1$. Expected pairs of quasars must constitute $\lesssim 10\%$ of the total number.

Regarding galaxies, the temperature in the layer from which galaxies presumably form is relatively stable at $\sim 10^4 K$; this is determined by the features of the recombination law and of the radiation from the optically thin gas. The gas radiates most when partially ionized, whence the emission is mostly in lines and in recombination radiation. After recombination, the emission decreases sharply. Here the temperature that the gas achieves depends weakly on the history and mass and formation time of the pancake. This temperature stability might well reflect the same scatter in the density of galaxies from the average density.

15.6 Galaxy Rotation

Is the emergence of rotation possible in a theory if the initial perturbs are vortex-free? The Kelvin-Helmholtz theorems say that gravitational forces and radiative pressure are capable during the RD stage of creating only a potential-type velocity field, i.e., a field with zero vorticity. Before recomb, the density and pressure are uniquely related to each other and the pressure forces do not give rise to vortex motion. Finally, viscosity does not give rise to vorticity in potential-type motion.

In principle, the emergence of vortex motion is not excluded when potential-type motion leads to shock waves. However, the effect is likely to be small and we conclude that adiabatic perturb theory probably leads to vortex-free motion at recombination.n.

The second aspect of the question concerns the relation between the body's angular momentum and its vorticity. The problem of the emergence of angular momentum in vortex-free motion is connected with violation of axial symmetry or to variable density. A general property of rigid-body rotation is that it represents motion with a minimum KE for a given total angular momentum, so that a body isolated from external forces tends to rigid-body rotation as time passes, absent internal sources of energy. But rigid-body rotation is vortex motion. Viscosity evidently must give rise to a transition from potential-type motion with angular momentum to rigid-body rotations; i.e., the viscosity must give rise to vorticity. It does so by transforming into heat the surplus of KE exceeding the energy of rigid-body rotation with the same ang mom. Vorticity arises first at the boundary and gradually encompasses the whole volume.

Further discussion is now necessary of the theorem of the conservation of vorticity and the relation between

vorticity and ang mom. Three situations will be considered to explain how rotation might arise in galaxies and clusters.

A. Early Postrecombination Period of Small Adiabatic Perturbs

If we take account of the deviation of the density from the average value, then in the approximation quadratic with respect to perturb amplitude, the ang mom of a sphere differs from zero. For a density perturb amplitude of order $\delta_\rho/\rho \sim 1$, the speed is $u \sim l/t$, where l is the scale of the motion and t is the cosmological time. Thus

$$AngMom \sim \delta_\rho \times u \times l^4 \sim \rho \times l^5/t. \quad (42)$$

Substituting $t = (6\pi \times G \times \rho)^{1/2}$ yields

$$AngMom = G^{1/2} \times \rho^{3/2} \times l^5 \sim G^{1/2} \times M^{3/2} \times l^{1/2}, \quad (43)$$

where $M = \rho \times l^3$. But this is just the ang mom for which the centrifugal force keeps the mass M in a disk of size l .

B. Shock-Wave Induced Compression of the Cooled Gas at $z < z_c$, after Recombination

In the nonlinear picture, perturb evolution leads to strong shocks; in this situation conservation of vorticity no longer holds. Formally, this is connected with the growing entropy of the shock. When, after the shock passes, the gas cools from about $4 \times 10^5 K$ to $10^4 K$, its vorticity is not conserved. In one example, a shock wave coinciding with the plane $x = 0$ compressed the gas by a factor of 4, so that the motion parallel to the x axis is slowed by this factor behind the wave front. Examination of the governing equations shows that the compensation effect expressed by the equation $\partial u_y/\partial x - \partial u_x/\partial y = 0$, which leads to vortex-free motion before the shock compression, is completely absent after the compression. A rough approach then gives the estimate $\nabla \times u = H \times \rho / Avg(\rho)$, where H is the Hubble parameter at the time of compression. This is based on the nonlinear compression when the gradients of the velocity perturbs in one direction locally exceed the Hubble parameter. For a particular set of values, this leads to an angular velocity and rotation period of

$$\nabla \times u = 1/[7.5 \times 10^5 \text{ yr}] \text{ and } \tau = \pi / [Abs(\nabla \times u)] = 2.3 \times 10^6 \text{ yr}.$$

But this rotation period is 100 times less than what is observed!

C. Gravitational Interactions of Discrete Bodies

Consider now the last stage, when the perturbs lead to spatially separated discrete bodies interacting gravitationally. For point or spherical bodies, momentum could be exchanged, leading to changes in the direction and speed of motion. An irregularly shaped body has a nonzero quadrupole moment. This could lead to a change in the orbital angular momentum of both bodies upon encounters. Because part of the external field of a body with a quadrupole moment decreases as $1/r^3$, closest encounters with the other body dominate the interaction.

The torque acting on a given body with mass M_1 and quadrupole moment Q_1 due to a second body with Mass M_2 is of the order of

$$Abs[d(\text{ang.Mom.})/dt] \sim G \times Q_1 \times M_2 / r_{12}^3. \quad (44)$$

For passage at the impact parameter b^* , effectively $r_{12} = b^*$ and $t \sim b^*/u$, where u is the speed, so

$$Abs[\delta(\text{ang.Mom.})] \sim G \times Q_1 \times M_2 / [(b^*)^2 \times u] \quad (45)$$

A statistical estimate for chaotic collisions follows, leading to a rough result for the process of separating galaxies of

$$\delta(\text{ang mom}) = (G \times M^3 \times R)^{1/2}, \quad (46)$$

where M is the galactic mass and R is the galactic size. Note that this is just the ang mom necessary that the centrifugal force of mass M and radius R counterbalance the gravitational attraction force. An initial quadrupole moment could arise by the tidal effect of the second body on the first.

Begin here after August 31, presumably on September 15

15.7 Galactic Magnetic Fields

The origin of a galaxy's magnetic field is related to the dynamo effect, the strengthening of a field caused by the plasma motion. Previously believed insurmountable difficulties with the dynamo effect led to the proposal of a specific type of singularity and a comparatively strong primordial magnetic field frozen in the relic plasma. A galactic field of about 10^{-6} gauss is obtained by compression of the magnetic lines of force when the dilute gas condenses into galaxies. Between galaxies, a field of $\sim 10^{-9}$ gauss must remain. This formulation now appears artificial.

Consider therefore theories describing the generation of fields within a hot model of the Universe with no primordial field, but with small density and velocity perturbs

superposed on a homogeneous and isotropic Friedmann solution.

Conservation of ang mom for a sphere of radius R yields the condition

$$Ang\ mom = I \times w = (8\pi/15) \times \rho \times R^5 \times w = const \quad (47)$$

During the expansion, R grows, but the total density falls as $\rho \sim R^{-4}$ since the photon density dominates. Therefore the angular velocity decreases as $w \sim 1/R$ while the linear velocity $u = w \times R$ remains constant. The matter density decreases as $\rho \sim R^{-3}$. By virtue of ang mom conservation, therefore, as the expansion proceeds, the matter alone "would like" to rotate more slowly, with $w \sim R^{-2}$ and $U \sim 1/R$.

Under these conditions, the light electrons are dragged along by the radiation, but the heavy protons fall behind the rotation of the RD plasma. Given this difference, there arises an electric current and consequent magnetic field H directed along the rotation axis. But this in turn leads to an electromotive force that tends to equalize the electron and proton velocities. In the first approx, we assume that the two velocities differ little. We shall then find the values of H and dH/dt necessary so that the protons do not lag behind the electrons. Then we shall verify the difference between the velocities required for the creation of such a field is actually small. Analysis of the equations of motion for the protons leads to an asymptotic solution for the magnetic field

$$H = -2 \times m_p \times c \times w/e \quad (48)$$

In the vortex theory, the motion is examined for which the scale of the largest vortex equals the product of the velocity and the cosmological time, which is also the condition for the realization of turbulence. Thus $w \sim 2\pi/t$, where t is the cosmological time, which at recombination (or at the end of the RD period) is $\sim 3 \times 10^{12}$ s. With this value, we find that $H = 0.4 \times 10^{-15}$ gauss when $\rho_m \sim 3 \times 10^{-20}$ g/cm³. The density of matter in galaxies is less by $\sim 10^4$. If the expansion continues, then the frozen-in condition — the conservation of the magnetic flux — leads to a later decrease of H by an additional 10^2 to a value of 2×10^{-18} gauss.

A different mechanism leads to a still smaller value of 10^{-23} gauss

Thus the field due to rotation turns out to be quite small in comparison with that observed in the Galaxy, $\sim 10^{-6}$ gauss. A satisfactory solution of the galactic magnetic field problem is thus impossible without making use of the dynamo effect, which can produce exponential growth with time. Exact theorems on the impossibility of a dynamo have been proved for axisymmetric and planar motion.

One simple nonplanar situation illustrating rapid growth is the following: Imagine a torus with cross section S and radius R with a field H_0 . While preserving its volume, stretch the torus to a radius $2R$; the cross section decreases $\rho R/2$ but the field grows to $2H_0$ because of flux conservation. Now bend the torus into a figure eight and then fold the two rings into one torus. The linear dimensions return to the original, but the field is now $2H_0$. This operation can be repeated indefinitely, with exponential growth time if each cycle requires the same duration. One possible governing equation that gives rise to an exponential solution is

$$dH/dt = \nabla \times (\alpha H) \quad (49)$$

where "X" denotes the cross product. An absolute upper limit on the growth rate of the field is $e^{(wt)}$, where w is the angular velocity. With $w \sim 3 \times 10^8/yr$ and $t = 10^{10}yr$, such a law would give an increase of $e^{(300)}$, more than sufficient. "Only" $10^{10} - 10^{20}$ is needed.

There is no reliable theory, but neither is there a blind alley....

15.8 The Theory of Entropy Perturbations; & 15.9 The Vortex Theory

While explained in the text, I am skipping these topics in these notes because they are disfavored by the authors as explicitly stated at the end of Section 15.10: ...From this account it should be apparent that the present authors prefer the adiabatic theory of galaxy formation...

=====

15.10 A Comparison of the Evolutionary Theories of Galaxy Formation

The previously stated theoretical assertions are consequences of the initial conditions posited for an early time, lacking a theory for choosing these initial conditions. Very likely only one set of initial conditions, i.e., types of perturbations are likely, though this is a matter of personal taste.

In principle, this choice could be determined by comparing the evolutionary calculations with observational data about the characteristics of galaxies and clusters, as well as about the RR and nucleosynthesis.

The subsequent discussion about galaxy formation in this section will be based on all of the information developed previously in this book and that to be presented later, however inconvenient this may be.

Though at present there is no generally accepted theory, we will give our preference with the reasons behind that choice.

The first choice is that between processes involving the condensation of a dilute gas versus the explosion of a superdense body. The latter should not be confused with the overall expansion of the Universe, but rather the expansion of a "white hole." However, consider our own Galaxy, with a mass of $\sim 2 \times 10^{11} M_\odot$, and an ang. mom. of $\sim 2 \times 10^{74} gcm * 2/s$; this corresponds to a circular velocity of 300 km / s at a radius of 10 kpc. But if the Galaxy formed from an initially superdense body with a radius of $\sim 1pc$, the ang. mom. would have corresponded to a linear velocity at the equator greater than c , a glaring contradiction. Moreover, the body as a whole would have been inside its gravitational radius.

This objection is invalid with respect to quasars, because their ang. mom. is unknown. On the other hand, the whole idea of exploding white holes has the serious difficulty that the QM process of particle creation near the singularity leads to the early explosion of the white hole [???-LF] or to no explosion at all.

These remarks do not concern ideas about the present activity of quasars or galactic nuclei, though they limit the notions of a possible source of their energy.

Thus the viewpoint of galaxies arising from a dilute gas is dominant. Then the remaining question is the type of initial perturbs of the homogeneous and isotropic Friedmann model, i.e., between the galaxy formation theories set forth in the preceding sections.

To begin, consider perturbs near the singularity. Adiabatic and entropy perturbs are compatible with small metric perturbs, with a quasi- isotropic solution. Near the singularity therefore, such a solution is not distinguished by its local properties from a strictly isotropic and homogeneous solution, so the nucleosynthesis results are the same. In particular, the mass abundance results for He of $\sim .26$ and for D of less than .0001 are supported by observations,

The vortex theory requires a substantially anisotropic singularity, thereby changing the expansion law then. This leads to quite different nucleosynthesis results, probably disagreeing with observations: either > 0.3 for He or $\sim 2.5\%$ for D and 97.5% for H. To avoid the need for unusual initial conditions, it is much more plausible to assume that all types of perturbations are equally represented since a solution with a non-Friedmann-like beginning approaches a Friedmann form. In that case, vortex perturbs decay rapidly, entropy perturbs remain constant, and adiabatic perturbs grow. Thereafter, the evolution follows the tracks of the theory of perturbs.

Suppose we do not consider the period from the singularity until nucleosynthesis. Consider instead the later period from the end of e-e+ annihilation to the present. This is the period $10^8 > z > 0$, including the epochs of the RD plasma, He and H recombination, perturb growth in the neutral gas, structure formation, and the secondary ionization for the neutral gas not a part of gravitationally bound objects. Begin with a comparison

of the theory and RR observations.

A distinctive feature of the vortex theory is the assumption of a large perturb amplitude of a large velocity for the vortex motions superposed on the Hubble expansion. Another feature, unavoidable, is that vortex motion does not give rise to density perturbs immediately after recomb.

In one variant, it was assumed that the velocity of vortex motion at recomb is of the order of $0.1 - 0.4c$. The corresponding RR temperature fluctuations due to the Doppler effect are evidently $\Delta T/T = 0.1 - 0.4$. But what is observed is $\Delta T/T < 3 \times 10^{-4}$, and other effects could not have eliminated the incompatibility.

A slow motion variant with a comparatively low initial vortex velocity of $u/c \sim 0.03$ leads to effects that do not agree with the observed RR isotropy. And what about the attractiveness of the vortex theory? Is there not an element of arbitrariness? Are there other consequences?

To explain the current structure of the Universe via adiabatic perturbs, the metric perturbs must have an amplitude of order 0.001 to 0.0001 on a scale corresponding to a mass $M \sim 10^{13} - 10^{14} M_\odot$. One can continue the perturb spectrum smoothly with the same amplitude to higher and lower masses. Perturbs of longer wavelengths, corresponding to much higher masses, grow more slowly and result in $\delta\rho/\rho \ll 1$ today. They also produce RR perturbs of order 0.0001, which do not contradict observations. Perturbs corresponding to much lower masses decay and do not affect the creation of galaxies. If the amplitude of these perturbs is of order 0.001 to 0.0001, then upon decay no observable effects remain.

Thus in the adiabatic theory, one can choose an initial spectrum without any preferred scale by giving one characteristic quantity—the amplitude—and leaving the scale of galaxy clusters to the natural laws. The vortex theory lacks this simplicity, requiring a special choice of initial spectrum.

From this account, it should be apparent that the present authors prefer the adiabatic theory of galaxy formation.

Not discussed here is the entropy theory, which in recent years has been made more attractive through new observations and theoretical analysis.

15.11 Observational Data Concerning the Properties of Galaxies and Galaxy Clusters; The Average Density of Matter in the Universe

There are many sources of data, but the parameters of galaxies and clusters have not been well determined and error estimates are very subjective.

One parameter is the luminosity function, with the following cited by Peebles. Given MG as the absolute magnitude, then the average number of galaxies per unit volume brighter than MG is

$$n(< MG) = A \times 10^{al} \times MG \text{ with } al = 0.75 \text{ for } MG < MG^*$$

$$n(< MG) = B \times 10^{bt} \times MG \text{ with } bt = 0.25 \text{ for } MG > MG^*$$

For $MG = MG^*$, the two formulas must give the same answer, so

$$MG^* = -19.5 + 5 \log h_0,$$

$$\text{with } H_0 = 100 \times h_0 \text{ km/s/Mpc.}$$

To astronomers, the most reliable path to galaxy mass determination follows measurements of the rotation speed and their linear size via Newton's law for irregulars and spirals. For ellipticals, the masses can be determined via the dispersion in the line-of-sight star velocities. The mass function appears in Figure 52 and the overall mass contributions in Table 12.

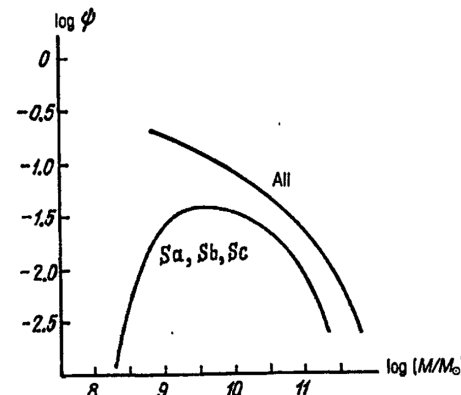


FIG. 52.—The mass function for galaxies of various types

TABLE 12
PERCENTAGE OF THE TOTAL MASS CONTRIBUTED BY
GALAXIES WITH VARIOUS MASSES

Percent contribution...	M₀/M			
	< 10 ⁹	10 ⁹ –10 ¹⁰	10 ¹⁰ –10 ¹¹	> 10 ¹¹
	3	11	40	46

The mass-to-luminosity ratio M/L in solar units is about 5 for irregulars and about 7-20 for spirals and about 40 for ellipticals.

Radio observations indicate that the rotation curves of most spirals are very flat: $V(R) = \text{const}$ to galactocentric distances of 50 kpc. Hence the cumulative (inner) mass satisfies

$$M(R) \sim V(R)^2 \times R \sim R$$

On the other hand, the spatial luminosity density in galaxy disks is well represented by an exponential model

$$I(a) = I_0 e^{(-a/a_0)},$$

So the cumulative luminosity

$$L(R) \sim \int_0^R I(a)a^2 da$$

converges rapidly to the total galaxy luminosity L_{tot} . The cumulative ratio $M(R) / L(R)$ has a value 3 -10 in solar units inside of the optically visible spiral boundaries depending on the stellar population.

The diameters of the brightest galaxies are $\sim 30\text{kpc}$, while dwarfs are much smaller. Galaxy angular momentum is known poorly.

The % distribution of galaxies by type is as follows:

TABLE II. Distribution of Galaxies by Type

E and S0	Sa.	Sb	Sc	Irr.	Others
22.9	7.7	27.5	27.3	2.1	12.5

Properties of galaxies are closely related to the properties of their respective systems. In rich clusters, most galaxies are type E or S0, explainable by the ram pressure of the intracluster gas. In poor clusters, ellipticals tend to populate inner regions; spirals and irregulars, the other regions.

The velocity dispersion of stars in the main galaxies of systems is equal to the main velocity dispersion of the galaxies, indicating that systems of galaxies form to-

gether with galaxies, since a later adjustment of dynamics takes too long.

The best studied clusters are regular clusters. For example, the size of the Coma is about 4 Mpc, with about an estimated several tens of thousands of galaxies. The velocity dispersion along the line-of-sight is about $\delta V = 1000\text{km/s}$, perhaps falling to half that value from the center to the edge of the cluster. By means of the viral theorem, one can estimate the cluster mass to be the very large $3 \times 10^{15} M_\odot / [H/(75\text{km/s/Mpc})]$

By counting the galaxies, one can determine the integrated luminosity and then the ratio M / L . One estimate is $300[H/(75\text{km/s/Mpc})]$, which is many times larger than the M/L for ellipticals, the type with the largest M/L . This signifies either (1) the cluster is nonstationary; (2) there is “invisible mass” between the visible parts of galaxies; or (3) there are systematic errors in the observations and their interpretations.

[The observations of Rubin et al. are neither mentioned nor cited!]

15.12 Astrophysical Consequences of the Existence of a Heavy Neutral Lepton